Higher-order hybrid implicit/explicit FDTD time-stepping

W. Tierens[a,*]

[a] *Max Planck Institut für Plasmaphysik*

Abstract

Both partially implicit FDTD methods, and symplectic FDTD methods of high temporal accuracy (3rd or 4th order), are well documented in the literature. In this paper we combine them: we construct a conservative FDTD method which is fourth order accurate in time and is partially implicit. We show that the stability condition for this method depends exclusively on the explicit part, which makes it suitable for use in e.g. modelling wave propagation in plasmas.

Keywords: FDTD, high order, partially implicit

1. Introduction

The Finite Difference Time Domain (FDTD) algorithm is a popular computational method for solving Maxwell's equations in time domain [12]. FDTD is explicit, and, like most explicit methods, it has a stability condition which puts an upper bound on the time step. Usually this condition is

$$c\Delta_t \leq \Delta/\sqrt{d} \tag{1}$$

where c is the speed of light, Δ_t the time step, Δ the space step (assuming cells of unit aspect ratio), and d the number of spatial dimensions.

Many attempts have been made to hybridise FDTD with stabler implicit methods, such that particular difficult sub-problems of limited size can be handled implicitly, while the overall algorithm retains the efficiency of explicit

*Corresponding author

Email address: wouter.tierens@ipp.mpg.de (W. Tierens)

FDTD. Sometimes this is done in the context of spatial refinement, where small features need to be resolved and the discretisation length must be (locally) small [4, 8, 2]. In other cases this is used to improve the behaviour of auxiliary differential equations which describe materials in the simulation.

Such hybrid methods are used to simulate electromagnetic waves in both magnetised and unmagnetised plasmas [10, 13, 11]. Thanks to this partially implicit approach, these algorithms remain stable at the vacuum stability condition even in dense plasmas.

Partially implicit FDTD algorithms have two main advantages

- Unlike fully explicit approaches, their stability condition is not sensitive to parameters of the implicit sub-problem.
- Unlike fully implicit approaches, the implicit equations have a structure which can be exploited to solve them efficiently (they are typically block-diagonal or banded, or of constant size).

Standard FDTD uses leapfrog time-stepping [12]. It is second-order accurate in time. Extending FDTD to third or fourth order accuracy in time is relatively straightforward: all it requires is making multiple leapfrog-like time steps with modified coefficients [6, 9, 7]. Doing so retains FDTD's symplecticity (a discrete energy remains exactly conserved).

In this paper, we will show how to construct a fourth-order accurate time stepping operator which is partially implicit: it retains the two main advantages listed above. We then apply this technique to simulate electromagnetic waves in unmagnetised plasmas.

In section 2, we construct a fourth-order accurate partially implicit time stepping operator, and show that it has the desired characteristics. Then in section 3, we apply our method to more realistic problems.

2. Constructing a fourth-order accurate hybrid implicit/explicit time stepping operator

2.1. In vacuum

As an introduction, let us first consider the vacuum case. Wave propagation is described by Maxwell's equations

$$\frac{\partial \vec{B}}{\partial t} = -\vec{\nabla} \times \vec{E} \tag{2}$$

$$\frac{\partial \vec{E}}{\partial t} = \frac{1}{\epsilon_0 \mu_0} \vec{\nabla} \times \vec{B} \tag{3}$$

which can be transformed in anti-symmetric form using $\vec{\mathcal{E}} = \sqrt{\epsilon_0}\vec{E}, \sqrt{\mu_0}\vec{\mathcal{B}} = \vec{B}$

$$\frac{\partial \vec{\mathcal{B}}}{\partial t} = -c\vec{\nabla} \times \vec{\mathcal{E}} \tag{4}$$

$$\frac{\partial \vec{\mathcal{E}}}{\partial t} = c\vec{\nabla} \times \vec{\mathcal{B}} \tag{5}$$

We wish to focus on temporal discretisation. Let us assume (without loss of generality) that only $\mathcal{E}_y$ and $\mathcal{B}_z$ are nonzero, and that they are proportional to $\exp(ikx)$

$$\frac{\partial \mathcal{B}_z}{\partial t} = ick\mathcal{E}_y \tag{6}$$

$$\frac{\partial \mathcal{E}_y}{\partial t} = ick\mathcal{B}_z \tag{7}$$

In matrix form

$$\frac{\partial}{\partial t} \begin{bmatrix} \mathcal{E}_y \\ \mathcal{B}_z \end{bmatrix} = \underbrace{\begin{bmatrix} 0 & ick \\ ick & 0 \end{bmatrix}}_{M} \begin{bmatrix} \mathcal{E}_y \\ \mathcal{B}_z \end{bmatrix} \tag{8}$$

The exact solution is

$$\begin{bmatrix} \mathcal{E}_y(t) \\ \mathcal{B}_z(t) \end{bmatrix} = \exp(Mt) \begin{bmatrix} \mathcal{E}_y(0) \\ \mathcal{B}_z(0) \end{bmatrix} \tag{9}$$

Note that the matrix M is anti-Hermitian. Its eigenvalues are therefore purely imaginary, and the eigenvalues of $\exp(Mt)$ lie on the unit circle for all t. This means that this eigenmode has a constant amplitude: it neither decays to zero, nor diverges to infinity, as time goes on. It is stable and lossless.

The most common way of discretizing (8) is the leapfrog approach

$$\begin{bmatrix} \mathcal{E}_y(t+\Delta_t) \\ \mathcal{B}_z(t+\frac{3}{2}\Delta_t) \end{bmatrix} = \underbrace{\begin{bmatrix} 1 & 0 \\ ick\Delta_t & 1 \end{bmatrix}}_{M_E} \underbrace{\begin{bmatrix} 1 & ick\Delta_t \\ 0 & 1 \end{bmatrix}}_{M_B} \begin{bmatrix} \mathcal{E}_y(t) \\ \mathcal{B}_z(t+\frac{1}{2}\Delta_t) \end{bmatrix} \tag{10}$$

$M_E M_B$ is indeed a second-order accurate approximation of (a staggered version of) $\exp(M\Delta_t)$. Its eigenvalues are also on the unit circle, conditional on Δ_t being sufficiently small:

$$\Delta_t \leq \frac{2}{c|k|} \tag{11}$$

If Δ_t obeys (11), $M_E M_B$ is stable and lossless, like the continuous case.

It was shown in [7, 6] that repeated steps of the form (10) with modified coefficients can be used to achieve better than second order accuracy. For example, third order accuracy is achieved using the following steps:

$$\begin{bmatrix} \mathcal{E}_y\left(t+\frac{1}{3}\Delta_t\right) \\ \mathcal{B}_z\left(t+\frac{1}{3}\Delta_t\right) \end{bmatrix} = \begin{bmatrix} 1 & 0 \\ \beta_1 ick\Delta_t & 1 \end{bmatrix} \begin{bmatrix} 1 & \alpha_1 ick\Delta_t \\ 0 & 1 \end{bmatrix} \begin{bmatrix} \mathcal{E}_y(t) \\ \mathcal{B}_z(t) \end{bmatrix} \tag{12}$$

$$\begin{bmatrix} \mathcal{E}_y\left(t+\frac{2}{3}\Delta_t\right) \\ \mathcal{B}_z\left(t+\frac{2}{3}\Delta_t\right) \end{bmatrix} = \begin{bmatrix} 1 & 0 \\ \beta_2 ick\Delta_t & 1 \end{bmatrix} \begin{bmatrix} 1 & \alpha_2 ick\Delta_t \\ 0 & 1 \end{bmatrix} \begin{bmatrix} \mathcal{E}_y\left(t+\frac{1}{3}\Delta_t\right) \\ \mathcal{B}_z\left(t+\frac{1}{3}\Delta_t\right) \end{bmatrix} \tag{13}$$

$$\begin{bmatrix} \mathcal{E}_y\left(t+\Delta_t\right) \\ \mathcal{B}_z\left(t+\Delta_t\right) \end{bmatrix} = \begin{bmatrix} 1 & 0 \\ \beta_3 ick\Delta_t & 1 \end{bmatrix} \begin{bmatrix} 1 & \alpha_3 ick\Delta_t \\ 0 & 1 \end{bmatrix} \begin{bmatrix} \mathcal{E}_y\left(t+\frac{2}{3}\Delta_t\right) \\ \mathcal{B}_z\left(t+\frac{2}{3}\Delta_t\right) \end{bmatrix} \tag{14}$$

where the coefficients are

$$\begin{aligned} \alpha_1 &= -1/24 & \beta_1 &= 1 \\ \alpha_2 &= 3/4 & \beta_2 &= -2/3 \\ \alpha_3 &= 7/24 & \beta_3 &= 2/3 \end{aligned} \tag{15}$$

It is straightforward to verify that (12-14) is indeed a third-order accurate approximation of $\exp(M\Delta_t)$.

2.2. In plasma

Wave propagation is described by Maxwell's equations coupled with a constitutive differential equation for every particle specie.

$$\frac{\partial \vec{\mathcal{B}}}{\partial t} = -c\vec{\nabla} \times \vec{\mathcal{E}} \tag{16}$$

$$\frac{\partial \vec{\mathcal{E}}}{\partial t} = -\sum_{s=1}^{N_s} \omega_s \vec{\mathcal{J}}_s + c\vec{\nabla} \times \vec{\mathcal{B}} \tag{17}$$

$$\frac{\partial \vec{\mathcal{J}}_s}{\partial t} = \omega_s \vec{\mathcal{E}} \tag{18}$$

where $\vec{\mathcal{J}}_s \omega_s \sqrt{\epsilon_0} = \vec{J}_s$, $\vec{J}_s$ is the current density associated with particle specie s, and the plasma frequency $\omega_s = \sqrt{\frac{n_s q_s^2}{m_s \epsilon_0}}$ is a function of the density n_s, charge q_s, and mass m_s. For simplicity we will assume that there is only one particle specie, $N_s = 1$.

Let us again assume (without loss of generality) that only $\mathcal{E}_y$ $\mathcal{J}_{1,y}$, $\mathcal{B}_z$ are nonzero, and that they are proportional to $\exp(ikx)$.

$$\frac{\partial}{\partial t}\begin{bmatrix} \mathcal{E}_y \\ \mathcal{J}_{1,y} \\ \mathcal{B}_z \end{bmatrix} = \underbrace{\begin{bmatrix} 0 & -\omega_1 & ick \\ \omega_1 & 0 & 0 \\ ick & 0 & 0 \end{bmatrix}}_{M_P} \begin{bmatrix} \mathcal{E}_y \\ \mathcal{J}_{1,y} \\ \mathcal{B}_z \end{bmatrix} \tag{19}$$

We again have an anti-Hermitian matrix, so the exact solution is stable and lossless. This time, we would like to approximate (19) in such a way that the stability condition does not depend on ω_1. Recall that the stability condition is the condition under which the eigenvalues of the time-stepping operator lie on the unit circle, like (11).

We proceed using a hybrid explicit/implicit approach, as in [10]. Let us first write the time-stepping equations

$$\frac{\mathcal{J}_{1,y}(t+\Delta_t)-\mathcal{J}_{1,y}(t)}{\Delta_t} = -\omega_1\frac{\mathcal{E}_y(t)+\mathcal{E}_y(t+\Delta_t)}{2} \tag{20}$$

$$\frac{\mathcal{B}_z\left(t+\frac{3}{2}\Delta_t\right)-\mathcal{B}_z\left(t+\frac{1}{2}\Delta_t\right)}{\Delta_t} = cik\mathcal{E}_y(t+\Delta_t) \tag{21}$$

$$\underbrace{\frac{\mathcal{E}_y(t+\Delta_t)-\mathcal{E}_y(t)}{\Delta_t}}_{\substack{\text{Time derivative}\\ \text{at } t+\frac{\Delta_t}{2}}} = \underbrace{\omega_1\frac{\mathcal{J}_{1,y}(t)+\mathcal{J}_{1,y}(t+\Delta_t)}{2}}_{\substack{\text{Implicit term}\\ \text{at } t+\frac{\Delta_t}{2}}} + \underbrace{cik\mathcal{B}_z\left(t+\frac{1}{2}\Delta_t\right)}_{\substack{\text{Leapfrog term}\\ \text{at } t+\frac{\Delta_t}{2}}} \tag{22}$$

It is (22) which mixes the explicit and implicit approaches. We see that there is a certain "compatibility" between the explicit and implicit terms: conceptually, they are both located at time $t+\frac{\Delta_t}{2}$. This may seem trivial, but we will later see that our fourth-order method has the same compatibility.

In matrix form

$$\begin{bmatrix} \mathcal{E}_y(t+\Delta_t) \\ \mathcal{J}_{1,y}(t+\Delta_t) \\ \mathcal{B}_z(t+\frac{3}{2}\Delta_t) \end{bmatrix} = \begin{bmatrix} 1 & 0 & 0 \\ 0 & 1 & 0 \\ ick\Delta_t & 0 & 1 \end{bmatrix} \begin{bmatrix} 1 & \frac{-\omega_1\Delta_t}{2} & 0 \\ \frac{\omega_1\Delta_t}{2} & 1 & 0 \\ 0 & 0 & 1 \end{bmatrix}^{-1} \cdot \begin{bmatrix} 1 & \frac{\omega_1\Delta_t}{2} & ick\Delta_t \\ \frac{-\omega_1\Delta_t}{2} & 1 & 0 \\ 0 & 0 & 1 \end{bmatrix} \begin{bmatrix} \mathcal{E}_y(t) \\ \mathcal{J}_{1,y}(t) \\ \mathcal{B}_z(t+\frac{1}{2}\Delta_t) \end{bmatrix} \tag{23}$$

The characteristic polynomial of this time-stepping operator is

$$-(\lambda-1)\left(\frac{\lambda\left(4c^2\Delta_t^2k^2+2\Delta_t^2\omega_1^2-8\right)}{\Delta_t^2\omega_1^2+4}+\lambda^2+1\right) \tag{24}$$

The first factor gives us the solution $\lambda = 1$, which is stable. The second factor is a palindromic polynomial [5] with real coefficients. This class of polynomials has roots either on the real line or on the unit circle. In this case, the roots are on the unit circle when $ck\Delta_t \leq 2$. The goal of having a ω_1-independent stability criterion was indeed achieved (in fact, this is the same stability criterion as (11)).

By repeatedly applying a step of the form (23), each with modified Δ_t, can we construct a high-order accurate approximation of $\exp(M_P\Delta_t)$, while retaining this desirable characteristic that the stability criterion is ω_1-independent?

One tempting possibility would be to use the same modified time steps as in the explicit case, e.g. using the coefficients (15). Alas, this does not work: The result does not approximate $\exp(M_P \Delta_t)$ to third order. We have attempted to calculate the correct coefficients α_i, β_i by demanding that the result approximates $\exp(M_P \Delta_t)$ to third order, but all solutions have complex α_i, β_i. The α_i, β_i need to be real in order to guarantee the unconditional stability of the implicit sub-problem (the $k = 0$ case). We therefore suspect that third-order accurate hybrid implicit-explicit time-stepping operators do not exist.

Somewhat surprisingly, this problem does not occur for the fourth-order accurate case. We use four ($i = 1, \cdots, 4$) sub-steps of the form (25). Demanding that the time-stepping operator approximates $\exp(M_P \Delta_t)$ to fourth order gives us a sensible solution with real α_i, β_i.

$$\begin{bmatrix} \mathcal{E}(t + \frac{i}{4}\Delta_t) \\ \mathcal{J}(t + \frac{i}{4}\Delta_t) \\ \mathcal{B}(t + \frac{i}{4}\Delta_t) \end{bmatrix} = \begin{bmatrix} 1 & 0 & 0 \\ 0 & 1 & 0 \\ cik\alpha_i\Delta_t & 0 & 1 \end{bmatrix} \begin{bmatrix} 1 & \frac{-\omega_1\beta_i\Delta_t}{2} & 0 \\ \frac{\omega_1\beta_i\Delta_t}{2} & 1 & 0 \\ 0 & 0 & 1 \end{bmatrix}^{-1} \cdot \begin{bmatrix} 1 & \frac{\omega_1\beta_i\Delta_t}{2} & cik\beta_i\Delta_t \\ \frac{-\omega_1\beta_i\Delta_t}{2} & 1 & 0 \\ 0 & 0 & 1 \end{bmatrix} \begin{bmatrix} \mathcal{E}(t + \frac{i-1}{4}\Delta_t) \\ \mathcal{J}(t + \frac{i-1}{4}\Delta_t) \\ \mathcal{B}(t + \frac{i-1}{4}\Delta_t) \end{bmatrix} \tag{25}$$

The coefficients are

$$\begin{aligned} \alpha_1 &= \tfrac{1}{6}\left(\sqrt[3]{2} + 2 + \tfrac{1}{\sqrt[3]{2}}\right) & \beta_1 &= 0 \\ \alpha_2 &= \tfrac{1}{6}\left(1 - \tfrac{1}{\sqrt[3]{2}} - \sqrt[3]{2}\right) & \beta_2 &= \tfrac{1}{3}\left(\sqrt[3]{2} + 2 + \tfrac{1}{\sqrt[3]{2}}\right) \\ \alpha_3 &= \tfrac{1}{6}\left(1 - \tfrac{1}{\sqrt[3]{2}} - \sqrt[3]{2}\right) & \beta_3 &= -\tfrac{1}{3}\left(1 + \sqrt[3]{2}\right)^2 \\ \alpha_4 &= \tfrac{1}{6}\left(\sqrt[3]{2} + 2 + \tfrac{1}{\sqrt[3]{2}}\right) & \beta_4 &= \tfrac{1}{3}\left(\sqrt[3]{2} + 2 + \tfrac{1}{\sqrt[3]{2}}\right) \end{aligned} \tag{26}$$

So the time-stepping proceeds as follows

- Step 1A: $\mathcal{E}$, $\mathcal{J}$ and $\mathcal{B}$ are known at time t_0. $\mathcal{E}$ and $\mathcal{J}$ do not change in this step since $\beta_1 = 0$.
- Step 1B: Update $\mathcal{B}$ explicitly. $\mathcal{B}$ is now known at $t_0 + \alpha_1\Delta_t$.
- Step 2A: Update $\mathcal{E}$ and $\mathcal{J}$ hybrid implicitly/explicitly from t_0 to $t_0 + \beta_2\Delta_t$. Note that the implicit midpoint for this procedure is at $t_0 + \beta_2\Delta_t/2$, which

equals $t_0+\alpha_1\Delta_t$, the point at which $\mathcal{B}$ is currently known: the implicit and explicit terms are "compatible" in the same sense as in the second-order case (see (22)).

- Step 2B: Update $\mathcal{B}$ explicitly to $t_0 + (\alpha_1 + \alpha_2)\Delta_t$.
- Step 3A: Update $\mathcal{E}$ and $\mathcal{J}$ hybrid implicitly/explicitly from $t_0 + \beta_2\Delta_t$ to $t_0 + (\beta_2 + \beta_3)\Delta_t$. Once again the terms are compatible.
- Step 3B: Update $\mathcal{B}$ explicitly to $t_0 + (\alpha_1 + \alpha_2 + \alpha_3)\Delta_t$.
- Step 4A: Update $\mathcal{E}$ and $\mathcal{J}$ hybrid implicitly/explicitly from $t_0+(\beta_2+\beta_3)\Delta_t$ to $t_0 + \Delta_t$. Once again the terms are compatible.
- Step 4B: Update $\mathcal{B}$ explicitly to $t_0 + \Delta_t$.

When $k = 0$, the sub-steps (25) reduce to fully implicit steps, and the time-stepping operator becomes unconditionally stable. What remains to be shown is that even when $k \neq 0$, the stability criterion does not depend on ω_1 (or at least that it is not more restrictive for large ω_1 than for small ω_1).

No matter the values of the coefficients α_i, β_i, the characteristic polynomial of this time-stepping operator is an anti-palindromic[5] polynomial with real coefficients.

$$c_{0,3} + c_{1,2}\lambda - c_{1,2}\lambda^2 - c_{0,3}\lambda^3 \tag{27}$$

$c_{0,3} = 1$, but $c_{1,2}$ is a complicated function of $\alpha_i, \beta_i, ck, \omega_1, \Delta_t$.

This polynomial can be factorised

$$-(-1+\lambda)(\lambda(1+c_{1,2}) + \lambda^2 + 1) \tag{28}$$

The solution $\lambda = 1$ is unconditionally stable. What remains is a second-order palindromic polynomial whose stability condition is given by

$$1 + c_{1,2} \in [-2, 2] \tag{29}$$

We have plotted this stability condition for $ck = 2$ in figure 1 (blue). It can be shown that in the $\omega_1 = 0$ (vacuum) case the stability condition is

$$c\Delta_t \leq \frac{\sqrt{12 - 6\ 2^{2/3}}}{|k|} \tag{30}$$

and in the $\omega_1 \to \infty$ (dense) case

$$c\Delta_t \leq \frac{2\sqrt{6 - \left(1 + \sqrt[3]{2}\right)^2}}{|k|} \tag{31}$$

The stability condition in the $\omega_1 \to \infty$ case is less restrictive than the stability condition in the $\omega_1 = 0$ case. The dense case is no less stable than the vacuum case. This is a highly desirable characteristic of partially implicit methods [10, 13, 11], and this fourth-order method retains this characteristic.

For comparison, figure 1 also contains the stability condition for the purely explicit fourth-order method (orange). Unlike the hybrid method, it becomes less and less stable as the plasma density increases.

3. Examples

The problem (16-18) can be discretized spatially and can then be brought under the block-matrix form

$$\frac{\partial}{\partial t}\begin{bmatrix} \mathbf{E} \\ \mathbf{J} \\ \mathbf{B} \end{bmatrix} = \begin{bmatrix} 0 & -\omega_p & cC \\ \omega_p & 0 & 0 \\ -cC^T & 0 & 0 \end{bmatrix}\begin{bmatrix} \mathbf{E} \\ \mathbf{J} \\ \mathbf{B} \end{bmatrix} \tag{32}$$

where C is a discrete curl matrix (e.g. on a Yee grid), ω_p is a diagonal matrix which has the (possibly location-dependent) plasma frequency on its diagonal, and $\mathbf{E}, \mathbf{J}, \mathbf{B}$ are row vectors containing the discretized $\mathcal{E}, \mathcal{J}, \mathcal{B}$ values. The reasoning of section 2 remains valid in the spatially discrete case, but k needs to be replaced by a discretized k_{discrete}. For the standard second-order Yee grid, $k_{\text{discrete}} = \frac{2}{\Delta} \sin\left(\frac{k\Delta}{2}\right)$.

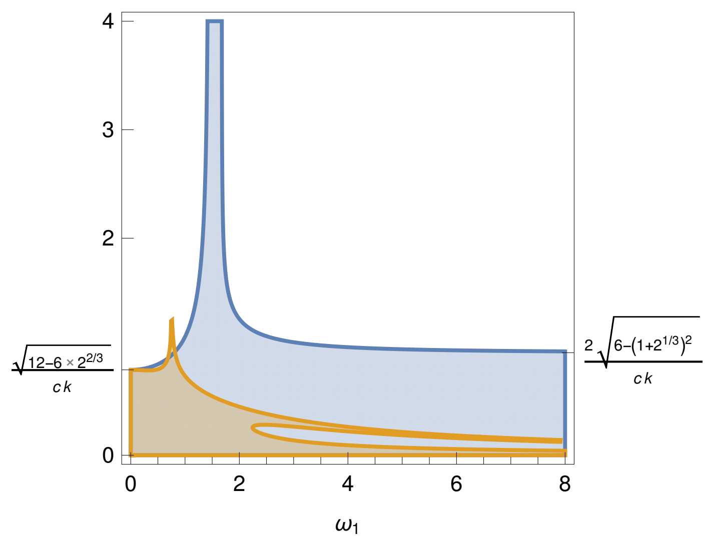

Figure 1: Area shaded in blue: parameters for which our fourth-order time-stepping scheme is stable, here plotted for $ck = 2$. Exact limiting conditions in the $\omega_1 = 0$ and $\omega_1 = \infty$ limits are also shown. Area shaded in orange: parameters for which a purely explicit fourth-order time-stepping scheme is stable.

3.1. Algorithm

We can time-step (32) using four sub-steps like (25)

$$\begin{bmatrix} \mathbf{E}_{\frac{i}{4}} \\ \mathbf{J}_{\frac{i}{4}} \\ \mathbf{B}_{\frac{i}{4}} \end{bmatrix} = \begin{bmatrix} I & 0 & 0 \\ 0 & I & 0 \\ -cC^T\alpha_i\Delta_t & 0 & I \end{bmatrix} \underbrace{\begin{bmatrix} I & \frac{\omega_p\beta_i\Delta_t}{2} & 0 \\ \frac{-\omega_p\beta_i\Delta_t}{2} & I & 0 \\ 0 & 0 & I \end{bmatrix}}_{M}^{-1} \cdot$$

$$\begin{bmatrix} I & \frac{-\omega_p\beta_i\Delta_t}{2} & cC\beta_i\Delta_t \\ \frac{\omega_p\beta_i\Delta_t}{2} & I & 0 \\ 0 & 0 & I \end{bmatrix} \begin{bmatrix} \mathbf{E}_{\frac{i-1}{4}} \\ \mathbf{J}_{\frac{i-1}{4}} \\ \mathbf{B}_{\frac{i-1}{4}} \end{bmatrix} \tag{33}$$

Because ω_p is diagonal, the matrix M, which is inverted in the above formula, is (up to permutation) a block-diagonal matrix with 2×2 blocks, and therefore easily invertible. This is another advantage of hybrid implicit/explicit methods: the overall algorithm is has the same asymptotic complexity as FDTD.

The spatial accuracy of this algorithm can be set by choosing a curl C of the desired order [3].

3.2. Dispersion

The dispersion relation for unmagnetised plasma is

$$k^2 = \frac{\omega^2 - \omega_1^2}{c^2} \tag{34}$$

In figure 2, we show the numerically determined dispersion relation and the exact dispersion relation. The numerical dispersion relation was determined as follows: we sent a wide-band waveform through 1D uniform plasma. We fourier transformed the resulting electric field (a function of x and t) in space and time, which gives us an amplitude vs k and ω. This amplitude has peaks where waves exist numerically, i.e. on the numerical dispersion curve. In the well-resolved limit, the analytical and numerical dispersion relations are almost equal.

3.3. Stability

Because k_{discrete} has an upper bound, we can identify the least stable mode (recall that the maximum stable time step for a single mode was inversely pro-

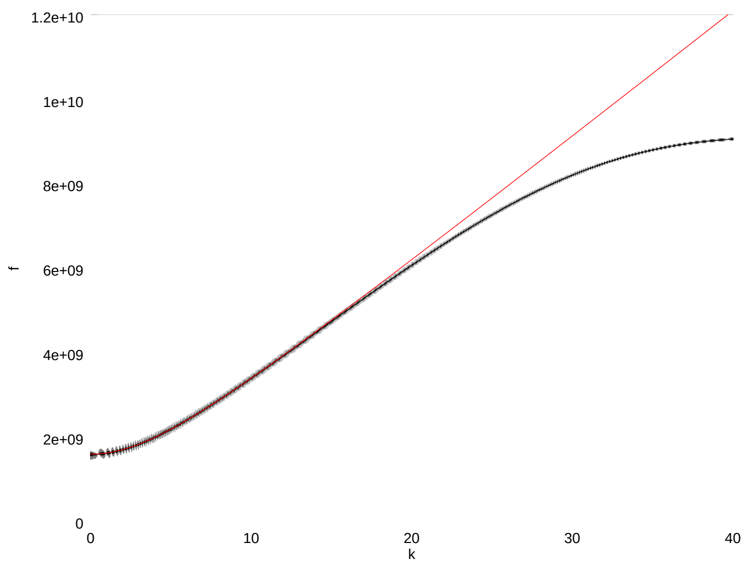

Figure 2: Gray: numerical discrete dispersion relation for our fourth-order method, obtained using a 2D fourier transform. Red: exact dispersion relation.

portional to k, see (30)), and write the stability condition for the whole algorithm

$$c\Delta_t \leq \frac{\sqrt{12 - 6\ 2^{2/3}}}{\max(k_{\text{discrete}})} \tag{35}$$

We have never observed instabilities with this upper bound for Δ_t.

In figures 3 and 4, we plot numerically determined eigenvalues of the time-stepping operator for a 1D configuration with 90 degrees of freedom (30 E_y, 30 B_z, 30 J_y). They all lie on the unit circle when (35) is obeyed. As the density increases, the eigenvalues migrate towards, but never quite reach, -1.

3.4. Energy conservation

Like standard second-order FDTD, our fourth-order scheme should conserve a discrete energy. For second-order FDTD in vacuum, the expression for the exact conserved discrete energy is known [1]. This exact conserved discrete energy approximates, but does not equal, the continuous electromagnetic energy

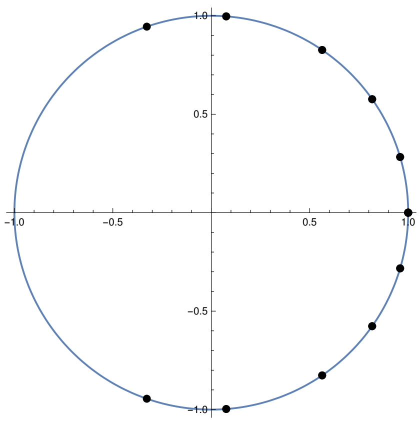

Figure 3: Eigenvalues of fourth-order time stepping operator in vacuum.

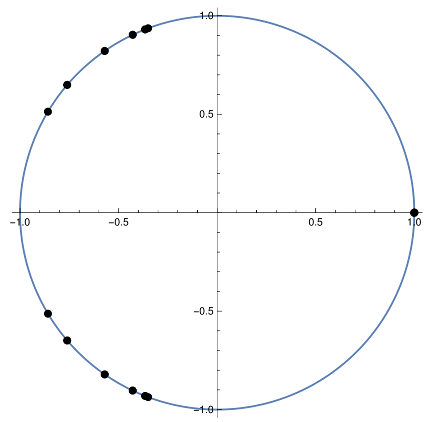

Figure 4: Eigenvalues of fourth-order time stepping operator in plasma.

(36)

$$E_{\text{total}} = \int_{\text{space}} \left(\frac{\epsilon_0}{2} E^2 + \frac{1}{2\mu_0} B^2 \right) dV \tag{36}$$

In plasma the energy is

$$E_{\text{total}} = \int_{\text{space}} \left(\frac{\epsilon_0}{2} E^2 + \frac{1}{2\mu_0} B^2 + \sum_s \frac{1}{2} n_s m_s v_s^2 \right) dV \tag{37}$$

where the third term is the kinetic energy of the particles.

The exact conserved discrete energy may be hard to determine even when it exists. For this reason, it is common to calculate and plot the continuous electromagnetic energy[6, 1]. This is not exactly constant even for conservative algorithms, but for conservative algorithms it always oscillates around a constant value. We have plotted the continuous energy (37) for the second-order method and for the fourth-order method in figure 5. We initialised our algorithm with random $\mathbf{E}, \mathbf{J}, \mathbf{B}$ (the same in both cases) and ran for 7000 steps. In both cases, energy is conserved. For the fourth-order method, the amplitude of the energy oscillations is much smaller. This is typical, see [6].

3.5. Transmission through a plasma layer

As another example, we consider 1D propagation through a layer of plasma. Here a plasma slab of width 2m and $\omega_p = 10^9$Hz is used. Other relevant

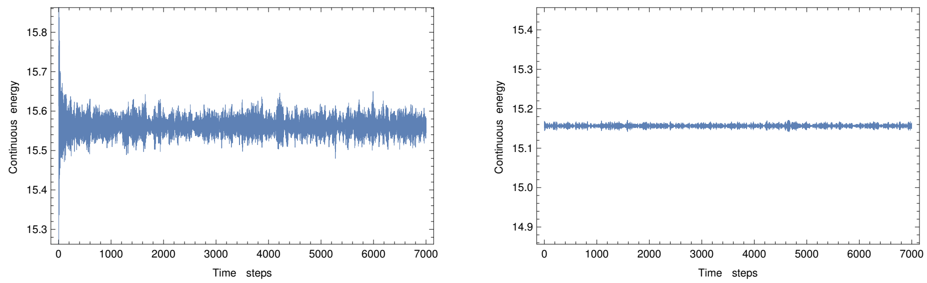

Figure 5: Conservation of energy for the second-order method (left) and for the fourth-order method (right).

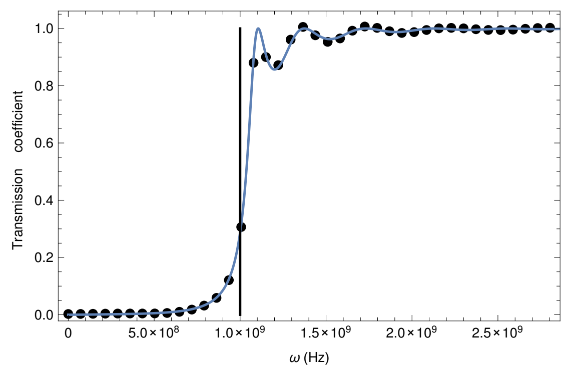

Figure 6: Exact (blue line) and numerical (black dots) transmission coefficients for waves propagating through a layer of plasma. The black vertical line indicates the plasma frequency.

parameters are $\Delta = 1\text{cm}$ and $\Delta_t = 1.74 \cdot 10^{-11}\text{s}$ calculated from (35). No absorbing boundary conditions were used, the simulation region was simply chosen large enough so that the waves do not reach the edges.

We used our fourth-order accurate method (fourth order in space and time) to calculate the transmission coefficient vs. the wave frequency, by transmitting a Gaussian pulse and Fourier transforming the results. This is shown in figure 6. Low frequencies are blocked, high frequencies are transmitted, as expected. The agreement with the theoretical result is excellent.

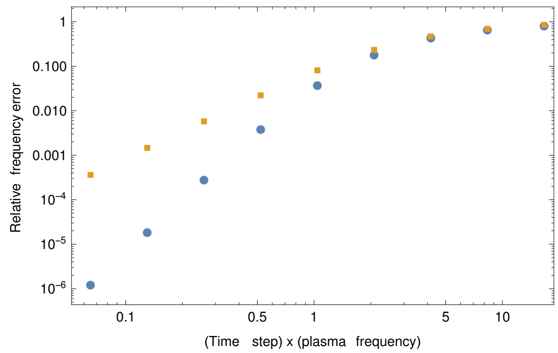

Figure 7: Error on the numerically determined fundamental frequency of a cylindrical plasma-filled cavity, determined with the second-order (orange) and fourth-order (blue) methods.

3.6. Fundamental eigenmode of a plasma-filled cylindrical cavity

Let us now consider a 2D example. We attempt to calculate the fundamental frequency of a plasma-filled cylindrical cavity with height $H = 0.2$m and radius $r = 0.2$m, filled with plasma with $\omega_1 = 10^{12}$Hz. Assuming no variation in the ϕ direction, we discretize this problem on a 20×20 grid with $\Delta = 1$cm, and we use the second-order accurate dicrete curl operator in cylindrical coordinates.

The exact fundamental frequency for this configuration is $1.00003 \cdot 10^{12}$Hz. The corresponding period is too short to be well-resolved when Δ_t is chosen based on the vacuum stability condition. As we shrink Δ_t, the numerically determined fundamental frequency becomes more and more accurate, as shown in figure 7. The accuracy for the fourth-order method increases faster than for the second-order method, as expected. The fundamental eigenmode itself is shown in figure 8.

4. Conclusion

In this paper, we have constructed a partially implicit FDTD method that is fourth order accurate in time (it can be fourth order in space as well if fourth-order curl stencils are used). Our method has several desirable characteristics

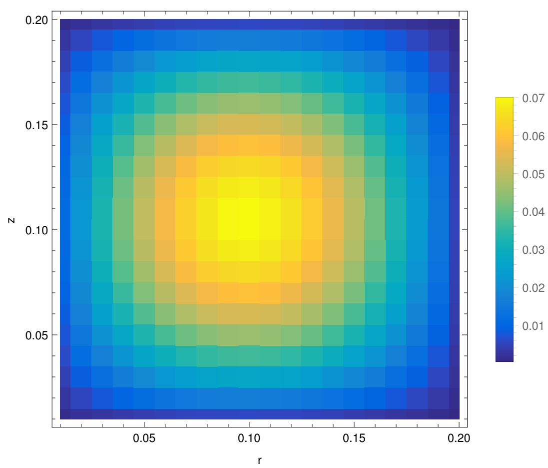

Figure 8: E_ϕ for the fundamental eigenmode in the plasma-filled cylindrical cavity.

in common with second-order partially implicit FDTD methods: the stability condition does not depend on parameters of the implicit sub-problem, and the overall algorithm has the same asymptotic complexity as FDTD.

We have shown that this algorithm is capable of modelling wave propagation in cold unmagnetised plasmas, an area where partially implicit techniques are necessary to avoid excessively restrictive stability conditions in dense plasmas [10, 13, 11]. Our algorithm can likely be extended to work in magnetised plasmas as well.

[1] R. A. Chilton. *H-, P- and T-refinement strategies for the finite-difference-time-domain (FDTD) method developed via finite-element (FE) principles.* PhD thesis, Ohio State University, 2008.

[2] B. De Deckere, A. Van Londersele, D. De Zutter, and D. Vande Ginste. Birefringent dispersive fdtd subgridding scheme. *Electronics Letters*, 52(17):1455–1457, 2016.

[3] Stavros V Georgakopoulos, Craig R Birtcher, Constantine A Balanis, and Rosemary A Renaut. Higher-order finite-difference schemes for electromag-

netic radiation, scattering, and penetration. 1. theory. *IEEE Antennas and Propagation Magazine*, 44(1):134–142, 2002.

[4] A. Van Londersele, D. De Zutter, and D. Vande Ginste. A new hybrid implicit-explicit FDTD method for local subgridding in multiscale 2D-TE scattering problems. *IEEE Transactions on Antennas and Propagation*, PP(99):1–1, 2016.

[5] I. Markovsky and S. Rao. Palindromic polynomials, time-reversible systems, and conserved quantities. *16th Mediterranean Conference on Control and Automation*, 2008.

[6] R Rieben, D White, and G Rodrigue. High-order symplectic integration methods for finite element solutions to time dependent maxwell equations. *IEEE Transactions on Antennas and Propagation*, 52(8):2190–2195, 2004.

[7] R. D. Ruth. A canonical integration technique. *IEEE Transactions on Nuclear Science*, 30(4):2669–2671, Aug 1983.

[8] T. Rylander and A. Bondeson. Stability of explicit–implicit hybrid time-stepping schemes for maxwell's equations. *Journal of Computational Physics*, 179(2):426–438, 2002.

[9] WEI Sha, Zhixiang Huang, Mingsheng Chen, and Xianliang Wu. Survey on symplectic finite-difference time-domain schemes for maxwell's equations. *IEEE Transactions on Antennas and Propagation*, 56(2):493–500, 2008.

[10] D. N. Smithe. Finite-difference time-domain simulation of fusion plasmas at radiofrequency time scales. *Physics of Plasmas*, 14(14):2537–2549, Apr. 2007.

[11] M. Surkova, W. Tierens, I. Pavlenko, D. Van Eester, G. Van Oost, and D. De Zutter. 3-D discrete dispersion relation, numerical stability, and accuracy of the hybrid fdtd model for cold magnetized toroidal plasma. *IEEE Transactions on Antennas and Propagation*, 62(12):6307–6316, 2014.

[12] A. Taflove and S. Hagness. *Computational Electrodynamics: The Finite-Difference Time-Domain Method*. Artech House, 2005.

[13] Y. Yu. An E-J collocated 3-D FDTD model of electromagnetic wave propagation in magnetized cold plasma. *IEEE transactions on Antennas and Propagation*, 58(2):469–478, 2010.